

# Analytical expressions for thermophysical properties of solid and liquid tungsten relevant for fusion applications

P. Tolias

*Space and Plasma Physics, Royal Institute of Technology, Stockholm, Sweden*

(Dated: November 19, 2018)

The status of the literature is reviewed for several thermophysical properties of pure solid and liquid tungsten that constitute important input for the modelling of intense plasma-surface interaction phenomena that are important for fusion applications. Reliable experimental data are analyzed for the latent heat of fusion, the electrical resistivity, the specific isobaric heat capacity, the thermal conductivity and the mass density from the room temperature up to the boiling point of tungsten as well as for the surface tension and the dynamic viscosity across the liquid state. Analytical expressions of high accuracy are recommended for these thermophysical properties that involved a minimum degree of extrapolations. In particular, extrapolations were only required for the surface tension and viscosity.

## I. INTRODUCTION

The survivability of the divertor during prolonged repetitive exposures to harsh edge plasma conditions as well as its longevity deep into the nuclear phase are essential for the success of the ITER project and impose stringent requirements on material selection [1]. After the decision that ITER will begin operations with a full tungsten divertor [2], R&D activities worldwide have focused on assessing various sources of mechanical and structural degradation of tungsten plasma-facing components in the hostile fusion reactor environment [3]; neutron irradiation effects on the mechanical properties, helium irradiation and hydrogen retention effects on the microstructure, thermal shock resistance and thermal fatigue resistance. The dependence of key mechanical properties (ductile to brittle transition temperature, yield strength, ultimate tensile strength, fracture toughness) on the fabrication history, the alloying or impurity elements, the metallurgical process and the grain structure is indicative of the complex nature of such investigations [4, 5]. As a consequence, the ITER Materials Properties Handbook puts strong emphasis to documenting the mechanical properties of tungsten [6].

Another phenomenon that is crucial for the lifetime of the tungsten divertor is melt layer motion during off-normal or transient events, namely edge localized modes, vertical displacement events and major disruptions [2]. Melt layer motion leads to strong modifications of the local surface topology and thus to degradation of power-handling capabilities but can also lead to plasma contamination by high-Z droplets in the case of splashing [7, 8]. The numerical modelling of melt motion is based on coupling the Navier-Stokes equations for the liquid metal with the heat conduction equation as well as the current continuity equation and supplementing the system with appropriate boundary conditions dictated by the incident plasma [9–11]. Therefore, the temperature dependence of the viscosity, surface tension and other thermophysical properties of liquid tungsten constitute a necessary input. Moreover, since re-solidification determines the onset but also the arrest of macroscopic motion, the thermophysical properties of solid tungsten at elevated temperatures and their behavior at the solid-liquid phase transition are also necessary input. Unfortunately, the ITER Materials Properties Handbook does not provide any information on the thermophysical properties of liquid tungsten and its recommended description of some thermophysical properties of solid tungsten at elevated temperatures is not based on state-of-the-art experimental data [6]. It should also be mentioned that these properties are also essential input for the modelling of tungsten dust transport [12, 13] (since tungsten dust should promptly melt in ITER-like edge plasmas and thermionic emission at the liquid phase plays a dominant role in its energy budget) and for the modelling of the interaction of transient plasmas with adhered tungsten dust [14] (since wetting is determined by the competition between the spreading and re-solidification rates).

This manuscript is focused on reviewing state-of-the-art measurements of several thermophysical properties of pure tungsten for temperatures varying from the room temperature up to the boiling point. The thermophysical properties of interest are the latent heat of fusion, the electrical resistivity, the specific isobaric heat capacity, the thermal conductivity and the mass density (for the solid and liquid phase) as well as the surface tension and the dynamic viscosity (for the liquid phase). The aim of the present investigation is to identify and critically evaluate reliable experimental datasets in order to propose accurate analytical expressions for the temperature dependence of these thermophysical properties. It has been possible to provide accurate analytical expressions for most properties based solely on experimental data and without the need for any extrapolations. The only exceptions are the surface tension and viscosity of liquid tungsten, where wide extrapolations had to be carried out beyond the melting point, since the only experimental sources on the temperature dependence referred to under-cooled liquid tungsten. These extrapolations are based on established empirical expressions that are known to be accurate for non-refractory liquid

metals and were cross-checked with constraints imposed by rigorous statistical mechanics relations. Taking into account that temperature gradients of the surface tension can be responsible for thermo-capillary flows and that viscosity is responsible for the damping of melt motion, it is important that such measurements are carried out in the unexplored temperature range, for instance with levitating drop methods on ground-based laboratories [15] or preferably in microgravity [16].

## II. THERMOPHYSICAL PROPERTIES OF TUNGSTEN

### A. The latent heat of fusion

The difference between the enthalpy of the liquid state and the enthalpy of the solid state at the melting transition yields the latent heat of fusion. In Table I, the values of the W latent molar heat of fusion are provided according to dedicated experiments [17–29], theoretical investigations [30–32] and material handbooks [33–37]. We point out that the measurement uncertainties in the determination of the heat of fusion with the resistive pulse heating (or dynamic pulse calorimetry) method can be expected to be around 10% [38]. Overall, given the uncertainties, the experimental data are well clustered around  $\Delta h_f \simeq 50$  kJ/mol. The value that is nearly exclusively cited in material handbooks and modelling works is  $\Delta h_f \simeq 52.3$  kJ/mol.

Some older literature sources quote a very small value  $\Delta h_f \simeq 35.3$  kJ/mol [39] which does not seem to be supported by any measurements. Most probably, this value stems from a semi-empirical relation known as Richard’s rule [40, 41]; By equating the liquid state with the solid state Gibbs free energy  $g = h - Ts$  at the melting point, we acquire  $\Delta h_f = T_m \Delta s_f$ . Richard’s rule states that the entropy of fusion is a quasi-universal constant for bcc and fcc metals with an approximate value  $\Delta s_f \simeq R$ , where  $R = N_A k_B$  is the ideal gas constant whose arithmetic value is  $R = 8.314$  J/(mol·K). This rule allows the calculation of  $\Delta h_f$  with knowledge of the melting temperature  $T_m$  only. For tungsten, we have  $T_m = 3695$  K, which translates to 30.72 kJ/mol. Modified versions of Richard’s rule take into account the average value of the entropy of fusion for all metals, which is  $\Delta s_f \simeq 1.15R$  [31] and indeed leads to the inaccurate prediction 35.3 kJ/mol for tungsten.

TABLE I: The latent molar heat of fusion for tungsten according to dedicated experiments, theoretical investigations and material handbooks.

Investigators	Reference	Year	Value (kJ/mol)	Details
Lebedev <i>et al.</i>	[17]	1971	54.9	Experimental (resistive pulse heating)
Martynyuk <i>et al.</i>	[18]	1975	54.4	Experimental (resistive pulse heating)
Shaner <i>et al.</i>	[19]	1976	46.0	Experimental (resistive pulse heating)
Seydel <i>et al.</i>	[20]	1979	50.6	Experimental (resistive pulse heating)
Bonnell	[21]	1983	53.0	Experimental (levitation calorimetry)
Arpaci & Frohberg	[22]	1984	50.3	Experimental (levitation calorimetry)
Berthault <i>et al.</i>	[23]	1986	46.7	Experimental (resistive pulse heating)
Senchenko & Sheindlin	[24]	1987	48.0	Experimental (resistive pulse heating)
Hixson & Winkler	[25]	1990	47.8	Experimental (resistive pulse heating)
Kaschnitz <i>et al.</i>	[26]	1990	47.1	Experimental (resistive pulse heating)
McClure & Cezairliyan	[27]	1993	48.7	Experimental (resistive pulse heating)
Pottlacher <i>et al.</i>	[28]	1993	52.4	Experimental (resistive pulse heating)
Kuskova <i>et al.</i>	[29]	1998	45.4	Experimental (resistive pulse heating)
Gustafson	[30]	1985	52.3	Modified experimental input for theory
Grimvall <i>et al.</i>	[31]	1987	52.3	Modified experimental input for theory
Dinsdale	[32]	1991	52.3	SGTE thermochemical database
Lassner & Schubert	[33]	1999	46.0	Handbook of material properties
Lide	[34]	2004	52.3	Handbook of material properties
Martienssen & Warlimont	[35]	2005	52.3	Handbook of material properties
Cardarelli	[36]	2008	52.3	Handbook of material properties
Shabalin	[37]	2014	52.3	Handbook of material properties

## B. The electrical resistivity

**Solid tungsten.** In 1984, Desai and collaborators managed to analyze all the 201 experimental datasets then available for the resistivity of tungsten [42]. A complete dataset covering the temperature range from the neighbourhood of the absolute zero up to 5000 K was synthesized from the most reliable measurements over different temperature intervals. For tungsten temperatures below the melting point, we shall be completely based on their analysis. In particular, we shall focus on the temperature range  $100 < T(\text{K}) < 3695$ . For the purpose of numerical manipulation, polynomial expressions were employed to acquire analytical fits for the electrical resistivity. The *Desai fit* reads as [42]

$$\rho = \begin{cases} +0.000015 + 7 \times 10^{-7}T^2 + 5.2 \times 10^{-10}T^5 & 1 \text{ K} \leq T \leq 40 \text{ K}, \\ +0.14407 - 1.16651 \times 10^{-2}T + 2.41437 \times 10^{-4}T^2 - 3.66335 \times 10^{-9}T^4 & 40 \text{ K} \leq T \leq 90 \text{ K}, \\ -1.06871 + 2.06884 \times 10^{-2}T + 1.27971 \times 10^{-6}T^2 + 8.53101 \times 10^{-9}T^3 - 5.14195 \times 10^{-12}T^4 & 90 \text{ K} \leq T \leq 750 \text{ K}, \\ -1.72573 + 2.14350 \times 10^{-2}T + 5.74811 \times 10^{-6}T^2 - 1.13698 \times 10^{-9}T^3 + 1.1167 \times 10^{-13}T^4 & 750 \text{ K} \leq T \leq 3600 \text{ K}, \end{cases}$$

where  $\rho$  is measured in  $10^{-8} \Omega\text{m}$  or in  $\mu\Omega\text{cm}$ . Note that the Desai fitting function is continuous at its branch points. The following remarks should be explicitly pointed out: **(i)** The uncertainty in the recommended values employed for the fit is estimated to be  $\pm 5\%$  below 100 K,  $\pm 3\%$  from 100 to 300 K,  $\pm 2\%$  from 300 to 2500 K,  $\pm 3\%$  from 2500 up to 3600 K,  $\sim \pm 5\%$  in the liquid region. **(ii)** The recommended polynomial fits do not necessarily imply a recommendation for the temperature derivative of the electrical resistivity. **(iii)** A large portion of the experimental datasets analyzed by Desai concern mono-crystalline specimens and many times the orientation of the single crystal is not even mentioned. It can be theoretically expected that the resistivity differences between monocrystalline and polycrystalline tungsten are insignificant, because of the bcc tungsten structure. In fact, this has been observed by Desai by inspecting the data. The synthesized Desai dataset was revisited by White and Minges in 1997 [43]. These authors fitted a fourth-order polynomial to the - corrected for thermal expansion - recommended values in the range  $100 < T(\text{K}) < 3600$ . The *White-Minges fit* reads as [43]

$$\rho = -0.9680 + 1.9274 \times 10^{-2}T + 7.8260 \times 10^{-6}T^2 - 1.8517 \times 10^{-9}T^3 + 2.0790 \times 10^{-13}T^4 \quad 100 \text{ K} \leq T \leq 3600 \text{ K},$$

where  $\rho$  is measured in  $10^{-8} \Omega\text{m}$  or in  $\mu\Omega\text{cm}$ . This polynomial fit is characterized by a 0.2% rms deviation as well as a maximum deviation of +0.6% at 150 K and -0.5% at 400 K. Finally, in the MIGRAINE dust dynamics code, the resistivity is also an input, since it is needed for the permittivity model that is employed in the Mie calculation of the emissivity. A polynomial fit was employed in the MIGRAINE code that is similar to the White-Minges expression. The *MIGRAINE fit* reads as [44]

$$\rho = +0.000015 + 1.52 \times 10^{-2}T + 1.2003 \times 10^{-5}T^2 - 3.3467 \times 10^{-9}T^3 + 3.7906 \times 10^{-13}T^4 \quad T \leq 3600 \text{ K},$$

where again  $\rho$  is measured in  $10^{-8} \Omega\text{m}$  or in  $\mu\Omega\text{cm}$ . A comparison between the resistivities and the resistivity temperature derivatives stemming from the three different fits can be found in figure 1. The deviations between the different fits are very small also for the temperature derivative. It is preferable though that the White-Minges fit is employed in future applications and extrapolated up to the actual melting point of 3695 K. The justification for the choice of this fit will be provided in the following paragraph.

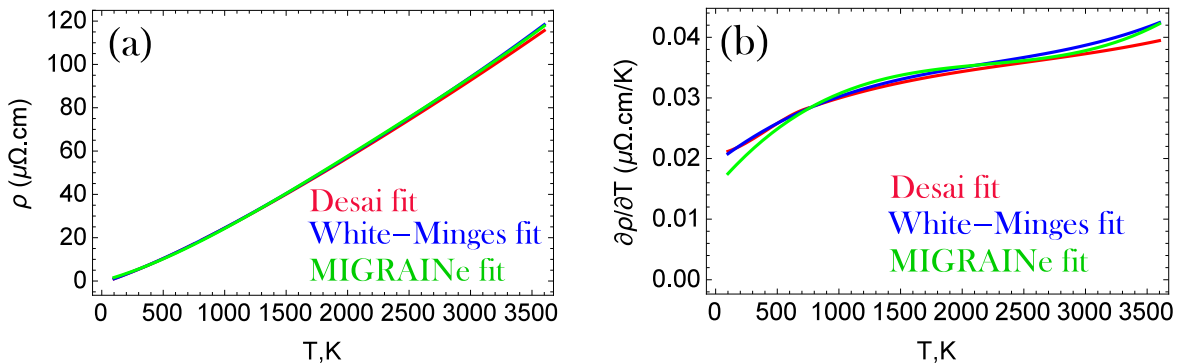


FIG. 1: (a) The tungsten resistivity as a function of the temperature according to three empirical analytical expressions. (b) The first temperature derivative of the tungsten resistivity as a function of the temperature according to these expressions.

TABLE II: The W electrical resistivity at the solid-liquid phase transition; the values from the solid and liquid side, as well as the discontinuity magnitude. The first two datasets [17, 18] have been corrected for thermal expansion following Ref.[42].

Investigators	Reference	Year	$\rho_s$ ( $\mu\Omega\text{cm}$ )	$\rho_l$ ( $\mu\Omega\text{cm}$ )	$\Delta\rho$ ( $\mu\Omega\text{cm}$ )
Lebedev <i>et al.</i>	[17]	1971	121	127	6
Martynyuk <i>et al.</i>	[18]	1975	118	125	7
Shaner <i>et al.</i>	[19]	1976	118	132	14
Seydel <i>et al.</i>	[20]	1979	120	137	17
Seydel & Fucke	[46]	1980	121	135	14
Desai <i>et al.</i>	[42]	1984	121	131	10
Berthault <i>et al.</i>	[23]	1986	123	138	15
Hixson & Winkler	[25]	1990	126	146	20
Kaschnitz <i>et al.</i>	[26]	1990	118	138	20
Pottlacher <i>et al.</i>	[28]	1993	126	145	19
Kuskova <i>et al.</i>	[29]	1998	120	140	20

**Discontinuity at the melting point.** The electrical resistivity of all elements has a discontinuity at the melting point. For most liquid metals  $\rho_l > \rho_s$  but there are few exceptions[45]. Reliable measurements of the W electrical resistivity asymptotically before and after the melting point have been outlined in Table II. Their mean values are  $\langle\rho_s\rangle \simeq 121\mu\Omega\text{cm}$  and  $\langle\rho_l\rangle \simeq 136\mu\Omega\text{cm}$ . They are very close to the measurements of Seydel & Fucke[46], whose measurements we are going to adopt not only for the discontinuity but also for the liquid state. The extrapolated value of the Desai fit is  $\rho_s \simeq 119\mu\Omega\text{cm}$ , the extrapolated value of the White-Minges fit is  $\rho_s \simeq 122\mu\Omega\text{cm}$  and the extrapolated value of the MIGRAINE fit is  $\rho_s \simeq 122\mu\Omega\text{cm}$ . Therefore, we conclude that the White-Minges fit (but also the MIGRAINE fit) can be extrapolated from 3600 K to 3695 K with a negligible error.

**Liquid tungsten.** The electrical resistivity of elemental liquid metals generally exhibits two tendencies [42, 45, 46]: (i) a monotonous increase beyond the melting point at a much slower pace than the solid state increase (e.g. refractory metals such as Ti, V, Mo), (ii) a very slow decrease right after the melting point followed by an increase again at a much slower pace than the solid state increase (e.g. the low melting point Zn). Tungsten belongs to the second group [46]. The experimental results have been fitted with a second-order polynomial. The *Seydel-Fucke fit* reads as

$$\rho = 135 - 1.855 \times 10^{-3}(T - T_m) + 4.420 \times 10^{-6}(T - T_m)^2 \quad T \geq 3695 \text{ K},$$

where  $\rho$  is measured in  $10^{-8}\Omega\text{m}$ . We point out that there are some uncertainties in the temperature measurements due to the lack of data for the temperature dependence of the liquid tungsten emissivity. A constant emissivity has been assumed across the liquid phase, which can be expected to translate from a 5%  $T$ -uncertainty near the melting point to a 10%  $T$ -uncertainty close to 6000 K. On the other hand, the uncertainties in the resistivity measurements should be 5 – 6%. To our knowledge, the only alternative analytical expression for the resistivity of liquid tungsten has been provided by Wilthan *et al.* [47], see also Refs.[48, 49]. The experiments were performed from 423 K to 5400 K and a polynomial fit was employed (including expansion effects). The *Wilthan-Cagran-Pottlacher fit* reads as [47, 48]

$$\rho = 231.3 - 4.585 \times 10^{-2}T + 5.650 \times 10^{-6}T^2 \quad T \geq 3695 \text{ K},$$

where again  $\rho$  is measured in  $10^{-8}\Omega\text{m}$  or in  $\mu\Omega\text{cm}$ . From figure 2, it is clear that the analytical fits are nearly identical.

**Recommended description.** The analytical description of the W electrical resistivity consists of employing the White-Minges fit in the temperature range  $100 < T(\text{K}) < 3695$  and the Seydel-Fucke fit in the temperature range  $3695 < T(\text{K}) < 6000$ . The W electrical resistivity is illustrated in figure 3. It is worth pointing out that the relative magnitude of the discontinuity of the resistivity at the liquid-solid phase transition is very small, whereas the relative magnitude of the discontinuity of the resistivity temperature derivative is very large (notice also the sign reversal).

### C. The specific isobaric heat capacity

**Solid tungsten.** The fourth and last edition of the NIST-JANAF Thermochemical Tables was published in 1998, but the tungsten data were last reviewed in June 1966 [50]. Measurements from 12 different sources were employed that were published from 1924 up to 1964. Only four of these datasets extend at temperatures beyond 2000 K, whereas five datasets are exclusively focused below the room temperature. The NIST webpage provides a Shomate equation

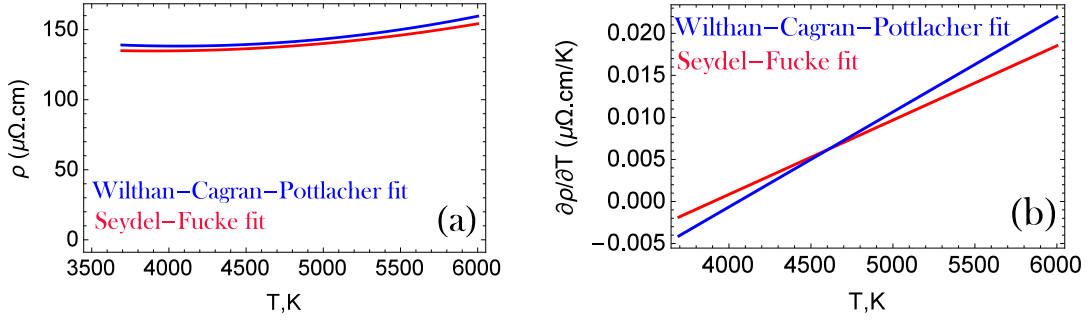


FIG. 2: (a,b) The tungsten resistivity & its first temperature derivative as a function of the temperature across the liquid state.

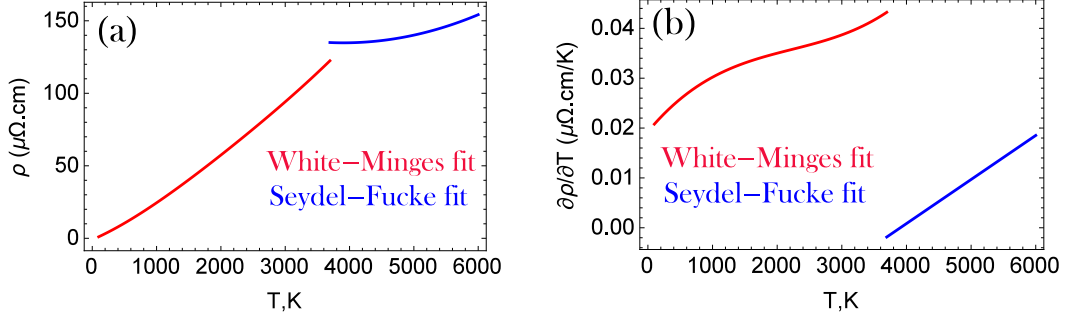


FIG. 3: (a,b) The recommended W electrical resistivity & its first temperature derivative for temperatures from 100 to 6000 K.

fit in the temperature intervals  $298 < T(\text{K}) < 1900$  and  $1900 < T(\text{K}) < 3680$ . The *NIST fit* reads as [51]

$$c_p = \begin{cases} +23.9593 + 2.63968 \times 10^{-3}T + 1.25775 \times 10^{-6}T^2 - 2.54642 \times 10^{-10}T^3 - \frac{4.8407 \times 10^4}{T^2} & 298 \text{ K} \leq T \leq 1900 \text{ K}, \\ -22.5764 + 9.02798 \times 10^{-2}T - 4.42715 \times 10^{-5}T^2 + 7.17663 \times 10^{-9}T^3 - \frac{2.40974 \times 10^7}{T^2} & 1900 \text{ K} \leq T \leq 3680 \text{ K}, \end{cases}$$

where  $c_p$  is measured in J/(molK). In 1997, White and Minges [43] revisited an earlier synthetic dataset of recommended values [52]. In the range above the room temperature, eleven datasets (dating up to 1994) were selected. The *White-Minges fit* reads as [43]

$$c_p = 21.868372 + 8.068661 \times 10^{-3}T - 3.756196 \times 10^{-6}T^2 + 1.075862 \times 10^{-9}T^3 + \frac{1.406637 \times 10^4}{T^2} \quad 300 \text{ K} \leq T \leq 3400 \text{ K},$$

where  $c_p$  is measured in J/(molK). This fit is characterized by a 1.1% rms deviation, the deviation from the mean is generally less than 1% below 1000 K and less than 2.5% above 1000 K. We point out that there are two misprints in the fitting expression as quoted in the original work [43]. As illustrated in figure 4a, the two expressions begin to strongly diverge above 2900 K; the high temperature measurements employed in the NIST fit are far less reliable.

**Liquid tungsten.** Measurements on free-electron-like elemental metals with low melting points [40] as well as recent experiments on elemental transition metals [28, 49] indicate that the enthalpy of liquid metals increases nearly linearly with the temperature over a wide range. In the case of liquid tungsten, the literature consensus is also that the enthalpy at constant pressure is a linear function of the temperature. This implies a constant isobaric heat capacity, courtesy of  $(\partial H/\partial T)_P = C_p$ . Thus, also the specific isobaric heat capacity  $c_p = \partial C_p/\partial m$  should be constant. However, there is a disagreement concerning the exact value: **(i)** The NIST-JANAF recommended value is  $c_p = 35.564 \text{ J/(molK)}$ . It is very outdated, being based on experiments that were carried out prior to 1961, *i.e.* many years before the dynamic pulse calorimetry or levitation calorimetry methods were developed. Unfortunately, this value is quoted in material property handbooks [33]. **(ii)** More reliable measurements provide values that are clustered around  $c_p = 52 \text{ J/(molK)}$ . We have  $c_p = 51.8 \text{ J/(molK)}$  [19],  $c_p = 57.0 \text{ J/(molK)}$  [20],  $c_p = 55.1 \text{ J/(molK)}$  [23],  $c_p = 48.2 \text{ J/(molK)}$  [25],  $c_p = 56.1 \text{ J/(molK)}$  [26],  $c_p = 52.9 \text{ J/(molK)}$  [28],  $c_p = 53.7 \text{ J/(molK)}$  [29]. Such deviations are justified in view of the fact that  $c_p$  is not directly obtained by the measurements but after post-processing (graphical determination from the slope of the enthalpy versus the temperature trace) and thus is subject to an uncertainty of around 10% [38]. **(iii)**



To our knowledge, the most modern experiments are those performed by Wilthan *et al.* [47] in 2005, who performed measurements up to 5400 K and found a constant liquid W value  $c_p = 51.3 \text{ J}/(\text{mol K})$ , that we shall adopt.

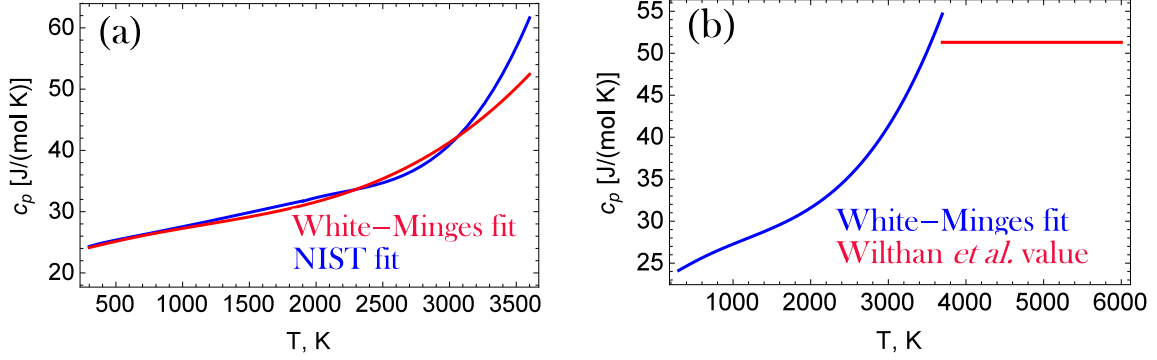


FIG. 4: (a) The W specific isobaric heat capacity in the solid state as a function of the temperature according to two empirical analytical expressions. (b) A complete analytical description of the W specific isobaric heat capacity from 300 to 6000 K by employing the White-Minges fit in the range  $300 < T(\text{K}) < 3695$  and the constant value of Wilthan *et al.*  $c_p = 51.3 \text{ J}/(\text{mol K})$  in the range  $3695 < T(\text{K}) < 6000$ .

**Recommended description.** (i) A complete analytical description of the tungsten specific isobaric heat capacity can be constructed by combining the White-Minges fit in the temperature range  $300 < T(\text{K}) < 3695$  and the constant value  $c_p = 51.3 \text{ J}/(\text{mol K})$  in the temperature range  $3695 < T(\text{K}) < 6000$ . See also figure 4b. This implies that the White-Minges fit needs to be extrapolated in the temperature range  $3400 < T(\text{K}) < 3695$ . This leads to  $c_p^s \simeq 54.7 \text{ J}/(\text{mol K})$  and thus to  $\Delta c_p \simeq 3.4 \text{ J}/(\text{mol K})$ . However, as can be observed in figure 4a, the heat capacity starts rapidly increasing at high temperatures, which implies that any extrapolation can lead to significant errors. (ii) Wilthan *et al.* have also provided an analytical fit for the tungsten enthalpy in the range  $2300 < T(\text{K}) < 3687$  [47]. Their fit reads as  $H(T) = 83.342 + 0.011T + 3.576 \times 10^{-5}T^2 \text{ (kJ/kg)}$ . It would be certainly preferable that the heat capacity was calculated from the local slopes of the experimental data, but here we have to differentiate the above fitting expression, which yields  $c_p = 11 + 7.152 \times 10^{-2}T \text{ [J/(kg K)]}$  or  $c_p = 2.022 + 1.315 \times 10^{-2}T \text{ [J/(mol K)]}$ . Therefore, we have  $c_p^s \simeq 50.6 \text{ J}/(\text{mol K})$  and thus  $\Delta c_p \simeq -0.7 \text{ J}/(\text{mol K})$ . (iii) Both results are physically acceptable; At the melting point, the difference in the heat capacity of metals between the solid and the liquid phases is rather small and it can be of either sign [40, 53]. (iv) In their common range of validity, the fits agree exceptionally well, see figure 5a, but they start diverging at both the interval endpoints. It is preferable to avoid any extrapolations and employ both fits. We shall first calculate their highest temperature intersection point, which is  $T \simeq 3080 \text{ K}$ . This allows us to connect the two fitting expressions in a continuous manner. The recommended description has the form

$$c_p = \begin{cases} 21.868372 + 8.068661 \times 10^{-3}T - 3.756196 \times 10^{-6}T^2 + 1.075862 \times 10^{-9}T^3 + \frac{1.406637 \times 10^4}{T^2} & 300 \text{ K} \leq T \leq 3080 \text{ K} \\ 2.022 + 1.315 \times 10^{-2}T & 3080 \text{ K} \leq T \leq 3695 \text{ K} \\ 51.3 & T \geq 3695 \text{ K} \end{cases}$$

where  $c_p$  is again measured in  $\text{J}/(\text{mol K})$ . The recommended analytical description is illustrated in figure 5b.

#### D. The thermal conductivity

**Solid tungsten.** In 1972; Ho, Powell and Liley provided recommended and estimated thermal conductivity values for all elements with atomic numbers up to  $Z = 105$  [54, 55]. Recommended datasets were synthesized for 82 elements after the careful analysis of 5200 different sets of experimental measurements. Their recommended dataset for tungsten will not be employed for the determination of the fitting expression but will be employed for comparison with our recommended treatment. In 1984; Hust and Lankford critically analyzed all literature data on the thermal conductivity of four key metals (aluminium, copper, iron, tungsten) for temperatures up to melting as well as provided analytical fits based on theoretical descriptions [56]. Their analysis was later closely followed by White and Minges [43]. Intricate details of their analysis and their utilization of the residual resistivity ratio will not be discussed here, since they are important for the low temperature part of the thermal conductivity ( $\lesssim 100 \text{ K}$ ), which is not relevant for fusion applications. They utilized 13 datasets for their fit, which contain experimental results from 2 K up to 3000 K (only four datasets contained measurements above 2000 K). The basic ingredients of the *Hust-Lankford fit* for tungsten

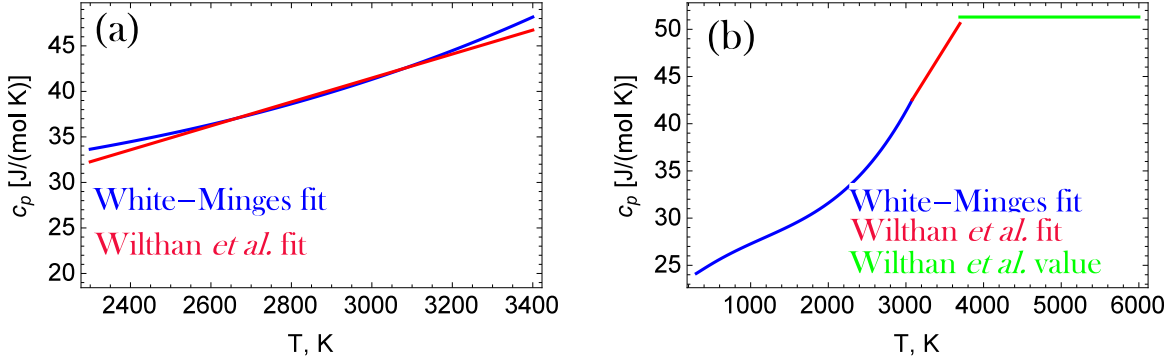


FIG. 5: (a) The specific isobaric heat capacity of solid state tungsten in the range  $2300 < T(\text{K}) < 3400$  according to two empirical analytical expressions. (b) The complete recommended analytical description of the W specific isobaric heat capacity from 300 to 6000 K.

are the electron-defect interaction term  $W_o$ , the electron-phonon interaction term  $W_i$  and the mathematical residual deviation term  $W_c$ . Their analytical expressions and their connection to the thermal conductivity read as [56]

$$W_c(T) = -0.00085 \ln\left(\frac{T}{130}\right) \exp\left\{-\left[\ln\left(\frac{T}{230}\right)\frac{1}{0.7}\right]^2\right\} + 0.00015 \exp\left\{-\left[\ln\left(\frac{T}{3500}\right)\frac{1}{0.8}\right]^2\right\} \\ + 0.0006 \ln\left(\frac{T}{90}\right) \exp\left\{-\left[\ln\left(\frac{T}{80}\right)\frac{1}{0.4}\right]^2\right\} + 0.0003 \ln\left(\frac{T}{24}\right) \exp\left\{-\left[\ln\left(\frac{T}{33}\right)\frac{1}{0.5}\right]^2\right\}, \\ W_i(T) = \frac{P_1 T^{P_2}}{1 + P_1 P_3 T^{(P_2+P_4)} \exp\left[-(P_5/T)^{P_6}\right]}, \quad W_o(T) = \frac{\beta}{T}, \quad k = \frac{1}{W_o(T) + W_i(T) + W_c(T)}.$$

The constant  $\beta$  has been chosen to correspond to a residual resistivity ratio of 300, whereas the  $P_i$  parameters were determined by least square fits of the combined dataset. Their arithmetic values are [56]

$$\beta = 0.006626, \quad P_1 = 31.70 \times 10^{-8}, \quad P_2 = 2.29, \quad P_3 = 541.3, \quad P_4 = -0.22, \quad P_5 = 69.94, \quad P_6 = 3.557.$$

Surprisingly, a comparison of the fit with the tabulated values reveals deviations below 90 K. This can either originate from misprints in the residual deviation  $W_c$  or from improper rounding-off of the least square coefficients. Since these deviations lie well below our temperature range of interest, we have not pursued this issue further. For completeness, the functional form of the tungsten thermal conductivity according to the Hust-Lankford fit is illustrated in figure 6. The plot covers the full temperature range of validity,  $2 < T(\text{K}) < 3000$ , but the fit will only be utilized in the temperature range  $300 < T(\text{K}) < 3000$ . In the latter range, the comparison with the Ho-Powell-Liley recommended dataset reveals a remarkable agreement. On the other hand, in the low temperature range, there are very strong deviations below 40 K (exceeding by far the selected plot scale). The emergence of these deviations is theoretically expected; they are a direct consequence of the electron-defect interaction term, which becomes dominant at very low temperatures and is a very sensitive function of the sample purity [57]. The Hust-Lankford fitting function is relatively cumbersome for numerical simulations. Its complexity stems from the low temperature maximum of the thermal conductivity, whose position lies well below fusion regimes of interest. An alternative empirical expression has been found by digitizing the Hust-Lankford fitting function with sampling steps of 50 K from 300 K to 3700 K and by least squares fitting the emerging dataset to the Shomate equation. This *modified Hust-Lankford fit* reads as

$$k = 149.441 - 45.466 \times 10^{-3}T + 13.193 \times 10^{-6}T^2 - 1.484 \times 10^{-9}T^3 + \frac{3.866 \times 10^6}{T^2},$$

where  $k$  is measured in W/(mK). The mean value of the absolute relative error is 0.39% and its maximum is 1.64%.

**Liquid tungsten.** (i) Experimental techniques that directly measure the thermal conductivity are based on formulas that are valid when heat conduction is the only viable mode of heat transfer. Their applicability to high temperature liquid metals such as tungsten is limited due to the increasing importance of convective and radiative heat transfer [58]. (ii) Experimental techniques that measure the thermal diffusivity  $\alpha = k/(\rho_m c_p)$  can clearly lead to the evaluation of the thermal conductivity [58]. However, post-processing requires the simultaneous knowledge of the mass density and the heat capacity and the measurement uncertainty can be large. (iii) Experimental techniques

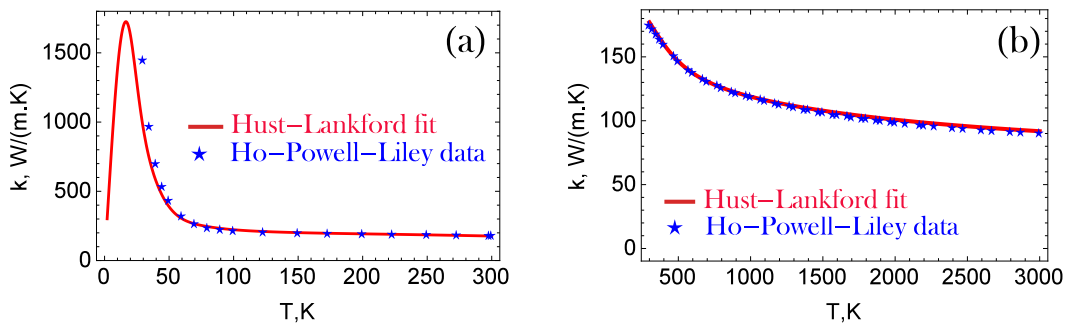


FIG. 6: The solid tungsten thermal conductivity. Comparison of the Hust-Lankford analytical fit [56] with the Ho-Powell-Liley [54, 55] recommended dataset in the (a) low temperature interval  $2 < T(\text{K}) < 300$ , where the deviations rapidly increase as  $T < 40 \text{ K}$ , (b) intermediate and high temperature interval  $300 < T(\text{K}) < 3000$ , where the agreement is excellent.

that measure the electrical resistivity  $\rho$  can also lead to the evaluation of the thermal conductivity [38, 45, 58, 59]. The connecting relation is the Wiedemann-Franz law, which, within the free electron theory of metals, has the form  $k_e = [(\pi k_B)/(\sqrt{3}e)]^2 (T/\rho)$ , where  $k_e$  denotes the electron thermal conductivity [60, 61]. The term in brackets is known as the Lorenz number and its nominal value is  $L_0 = 2.443 \times 10^{-8} \text{ W}\Omega\text{K}^{-2}$ . In metals, heat transport occurs through valence electron transport and lattice waves (phonons), *i.e.*  $k = k_e + k_{\text{ph}}$ . At high temperatures relevant for liquid tungsten, the first mechanism dominates [58]. Overall, we have  $k = L_0 T/\rho$ . (iv) In this manner, the abundance of liquid tungsten resistivity data, that have been acquired by dynamic pulse calorimetry, can be translated to thermal conductivity data. The use of the  $\rho(T)$  fitting expressions with the Wiedemann-Franz law can lead to the propagation of numerical errors. Therefore, when possible, it is preferable that first each resistivity data point is translated to thermal conductivity and that afterwards curve fitting takes place. This procedure has been followed for the Seydel and Fucke measurements [46]. In the original publication, the authors only provide the fitting expression for the resistivity, but their resistivity data have been presented in graphical form in Ref. [47]. The data have been extracted with the aid of software, they are represented by the average of three different extractions in order to avoid errors due to axis mismatch. The measurements consist of 13 datapoints from the melting temperature up to 6000 K and have been fitted with a quadratic polynomial. The *Seydel-Fucke fit* reads as

$$k = 66.6212 + 0.02086(T - T_m) - 3.7585 \times 10^{-6}(T - T_m)^2 \quad 3695 \text{ K} \leq T \leq 6000 \text{ K},$$

where  $k$  is measured in  $\text{W}/(\text{m K})$ . The mean value of the absolute relative fitting error is 0.25%, see also figure 7a. Let us compare with the measurements of Pottlacher from melting up to 5000 K [62]. The *Pottlacher fit* reads as [62]

$$k = 6.24242 + 0.01515T \quad 3695 \text{ K} \leq T \leq 5000 \text{ K},$$

where  $k$  is measured in  $\text{W}/(\text{m K})$ . We point out that typical uncertainties in the indirect determination of the thermal conductivity with dynamic pulse calorimetry are  $\sim 12\%$  [38, 59]. The two fitting functions are plotted in figure 7b, in their common domain of definition. The deviations are acceptable being  $< 7\%$ . Moreover, we note that the Seydel-Fucke experiments are in better agreement with other recent measurements [63]. Finally, it is worth mentioning that Ho-Powell-Liley provide provisional values for the thermal conductivity of tungsten over its entire liquid range, from the melting up to the critical point [54, 55]. These values were estimated with the phenomenological theory of Grosse, which is based on an empirical hyperbolic relation for the electrical conductivity of liquid metals [64, 65]. As illustrated in figure 7a and expected due to the oversimplified theoretical analysis, these provisional values are not accurate.

**Recommended description.** In order to complete the description, it is necessary to verify that the extrapolation of the modified Hust-Lankford fit in the temperature range  $3000 < T(\text{K}) < 3695$  is viable. (i) We have confirmed that the extrapolated values lie very close to the Ho-Powell-Liley recommended dataset [54, 55], which features seven data-points in this range, see figure 8a. (ii) We have performed a comparison with the thermal conductivity resulting from the combination of the White-Minges fit for the electrical resistivity [43] with the Wiedemann-Franz law. The agreement was satisfactory. We also note that the two curves overlap when employing  $L_{\text{eff}} = 1.185L_0$  for the effective Lorenz number. (iii) Overall, the recommended description comprises of the modified Hust-Lankford fit in the temperature range  $300 < T(\text{K}) < 3695$  and the Seydel-Fucke fit in the temperature range  $3695 < T(\text{K}) < 6000$ . See figure 8b for an illustration. (iv) From the above, we have  $k^s \simeq 87.0 \text{ W}/(\text{m K})$  and  $k^l \simeq 66.6 \text{ W}/(\text{m K})$ . The resulting discontinuity at the liquid-solid phase transition is  $\Delta k \simeq 20.4 \text{ W}/(\text{m K})$ . The large relative magnitude of the discontinuity and the fact that  $k^s > k^l$  agrees with results from other refractory metals [58].



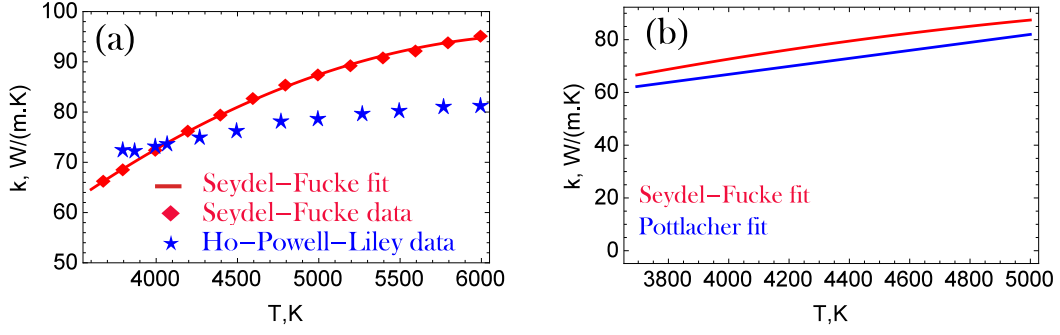


FIG. 7: (a) The liquid tungsten thermal conductivity in the range  $3695 < T(K) < 6000$ . The data of Seydel-Fucke [46, 47] (together with a quadratic fit) compared with the provisional values provided by Ho-Powell-Liley [54, 55]. (b) The thermal conductivity of liquid tungsten in the temperature range  $3695 < T(K) < 5000$  according to two empirical analytical expressions.

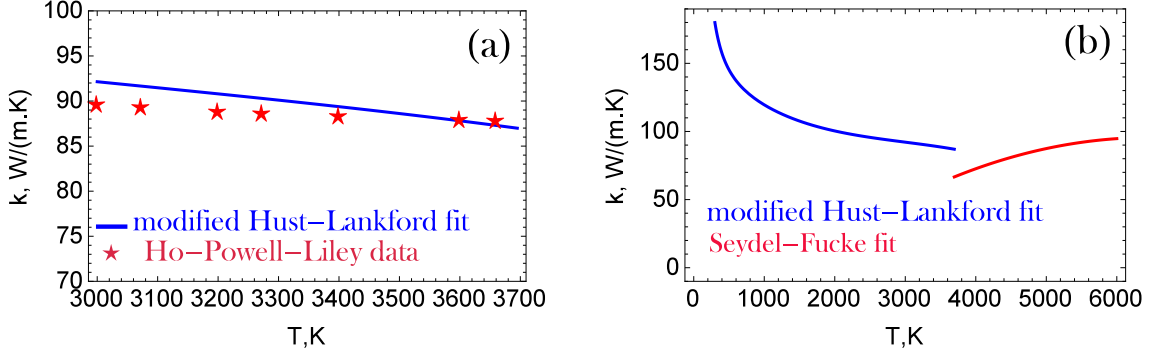


FIG. 8: (a) Extrapolation of the modified Hust-Lankford fit in the temperature range  $3000 < T(K) < 3695$  and comparison with the values recommended by Ho-Powell-Liley [54, 55]. (b) The complete recommended analytical description of the  $W$  thermal conductivity from 300 to 6000 K.

### E. The mass density

**Solid tungsten.** The analysis of White and Minges is based on a synthetic dataset constructed from eleven sets of measurements above 300 K and three sets of measurements below 300 K [43]. They provide a least-squares polynomial fit for the linear expansion coefficient  $\alpha_l = (1/l_0)(dl/dT)$ , where  $l_0$  is the length measured at the room temperature ( $T_0 = 293.15$  K), that is valid from 300 K up to 3500 K. The linear expansion coefficient fit reads as

$$\alpha_l = 3.873 + 2.562 \times 10^{-3}T - 2.8613 \times 10^{-6}T^2 + 1.9862 \times 10^{-9}T^3 - 0.58608 \times 10^{-12}T^4 + 0.070586 \times 10^{-15}T^5,$$

where  $\alpha_l$  is measured in  $10^{-6} K^{-1}$ . These authors only provide tabulated data for the relative change in the linear dimension  $\Delta l/l_0 = (l - l_0)/l_0$ . An analytical expression for the normalized linear dimension can either be calculated from the relation  $l/l_0 = 1 + \int_{T_0}^T \alpha_l(T')dT'$  or by least-squares fitting the tabulated data and employing  $l/l_0 = 1 + \Delta l/l_0$ . The normalized linear dimension fit reads as

$$\frac{l}{l_0} = 1 + 4.64942 \times 10^{-6}(T - T_0) + 2.99884 \times 10^{-11}(T - T_0)^2 + 1.95525 \times 10^{-13}(T - T_0)^3.$$

In the case of isotropic thermal expansion for a cubic metal such as tungsten, we have  $v/v_0 = (l/l_0)^3$  for the volume expansion. The specific volume fit reads as

$$\frac{v}{v_0} = 1 + 1.4016 \times 10^{-5}(T - T_0) + 4.4004 \times 10^{-11}(T - T_0)^2 + 6.3724 \times 10^{-13}(T - T_0)^3.$$

Finally, the dependence of the mass density of solid tungsten on the temperature can be evaluated by employing  $\rho_{m0} = 19.25 \text{ g cm}^{-3}$  for the room temperature mass density and  $v/v_0 = \rho_{m0}/\rho_m$  as imposed by mass conservation. The *White-Minges fit* reads as

$$\rho_m = 19.25 - 2.66207 \times 10^{-4}(T - T_0) - 3.0595 \times 10^{-9}(T - T_0)^2 - 9.5185 \times 10^{-12}(T - T_0)^3 \quad 300 \leq T(K) \leq 3400,$$

where  $\rho_m$  is measured in  $\text{g cm}^{-3}$ .

**Liquid tungsten.** So far we have employed the Seydel and Fücke measurements [46] for the electrical resistivity and the thermal conductivity of liquid tungsten. It would be consistent to employ the volume expansion data originating from the same experimental group, provided of course that they are reliable. (i) Seydel and Kitzel have provided thermal volume expansion data for five refractory metals (Ti, V, Mo, Pd, W) from their melting up to their boiling point [66]. They have successfully fitted the specific volume of tungsten to a quadratic polynomial. The *Seydel–Kitzel fit* reads as

$$\frac{v}{v_0} = 1.18 + 6.20 \times 10^{-5}(T - T_m) + 3.23 \times 10^{-8}(T - T_m)^2,$$

where  $v_0$  is the tungsten specific volume in room temperature. It is worth noting that the Seydel–Kitzel fit has been singled out as the recommended expression in specialized reviews [67]. (ii) Hixson and Winkler have measured the specific volume of liquid tungsten in the range  $3695 \leq T(\text{K}) \leq 5700$  [25]. They have provided linear expressions for the specific volume as a function of the enthalpy and for the enthalpy as a function of the temperature. Combining their expressions, we acquire the *Hixson–Winkler fit* that reads as

$$\frac{v}{v_0} = 0.83634 + 0.901 \times 10^{-4}T,$$

where  $v_0$  is the tungsten specific volume in room temperature. (iii) Kaschnitz, Pottlacher and Windholz have carried out similar measurements without providing fitting expressions [26]. However, the analytical fit of the specific volume as a function of the temperature has been plotted in a figure. We digitized this figure in the temperature range  $3695 \leq T(\text{K}) \leq 6000$  with steps of 100 K and we least-square fitted the resulting dataset to a quadratic polynomial. The *Kaschnitz–Pottlacher–Windholz fit* reads as

$$\frac{v}{v_0} = 1.184 + 5.27 \times 10^{-5}(T - T_m) + 1.17 \times 10^{-8}(T - T_m)^2,$$

where again  $v_0$  is the tungsten specific volume in room temperature. The mean value of the absolute relative fitting error is 0.05%. (iv) Hüpf *et al.* have also measured the volume expansion of five refractory liquid metals (V, Nb, Ta, Mo, W) [48]. We note that the authors provided a fit for the quantity  $D^2/D_0^2$  as a function of the temperature, where  $D$  denotes the wire diameter. Under rapid heating the melted wire expands solely in the radial direction, which implies that its volume is proportional to the cross-section and thus  $v/v_0 = D^2/D_0^2$  [59, 68]. The fitting expression consists of two polynomial branches, but it is continuous at the branch point. The *Hüpf fit* reads as

$$\frac{v}{v_0} = \begin{cases} 0.95062 + 6.344 \times 10^{-5}T & 3695 \leq T(\text{K}) \leq 5000, \\ 1.34989 - 1.0333 \times 10^{-4}T + 1.73957 \times 10^{-8}T^2 & 5000 \leq T(\text{K}) \leq 6000, \end{cases}$$

where again  $v_0$  is the tungsten specific volume in room temperature. The four fits are illustrated in figure 9a. It is evident that the Seydel–Kitzel fit greatly overestimates the volume expansion for very high temperatures with the deviations from the other curves starting from 4500 K. The cause of this overestimation was investigated in a seminal paper by Ivanov, Lebedev and Savvatimskii [68]; All the aforementioned experiments were based on the resistive pulse heating technique and the volume expansion measurements were carried out by recording the temporal evolution of the shadow the sample produced after illumination with a radiation source either in a dense gas or in a liquid. Only Seydel and Kitzel performed their experiments in water [66]. In that case, a layer of vapour surrounded the sample with its thickness determined by the sample temperature and its rapid evolution. Since vapor possesses a refractive index smaller than that of water, the vapor layer caused the shadow image to expand and was responsible for the overestimation. The correctness of the other fits was confirmed by the same authors by measurements of the thermal expansion of liquid tungsten with two alternative independent techniques, the capillary method and the probe method [66]. From figure 9a, it is also evident that, close to the melting point, the Hüpf fit deviates from the other curves. Combining the above and considering the more limited temperature range of the Hixson–Winkler fit, we conclude that the Kaschnitz–Pottlacher–Windholz fit is the most appropriate. It is preferable to convert this fit to an analytical expression for the mass density. Using  $\rho_{m0} = 19.25 \text{ g cm}^{-3}$  for the room temperature mass density of tungsten and  $v/v_0 = \rho_{m0}/\rho_m$ , we acquire the *Kaschnitz–Pottlacher–Windholz fit* for the mass density

$$\rho_m = 16.267 - 7.679 \times 10^{-4}(T - T_m) - 8.091 \times 10^{-8}(T - T_m)^2 \quad 3695 \leq T(\text{K}) \leq 6000,$$

where  $\rho_m$  is measured in  $\text{g cm}^{-3}$ . This fit is illustrated in figure 9. The density of liquid tungsten at the melting point is  $\rho_m^l = 16.267 \text{ g cm}^{-3}$ , which is very close to typical values recommended in handbooks.

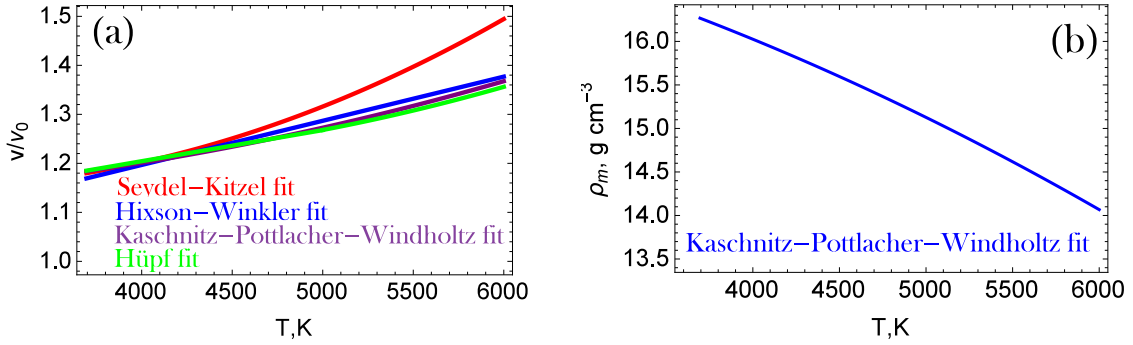


FIG. 9: (a) The liquid tungsten thermal volume expansion in the range  $3695 < T(\text{K}) < 6000$  according to four empirical analytical expressions [25, 26, 48, 66]. (b) The mass density of liquid tungsten in the range  $3695 < T(\text{K}) < 6000$  according to the Kaschnitz–Pottlacher–Windholtz fit [26].

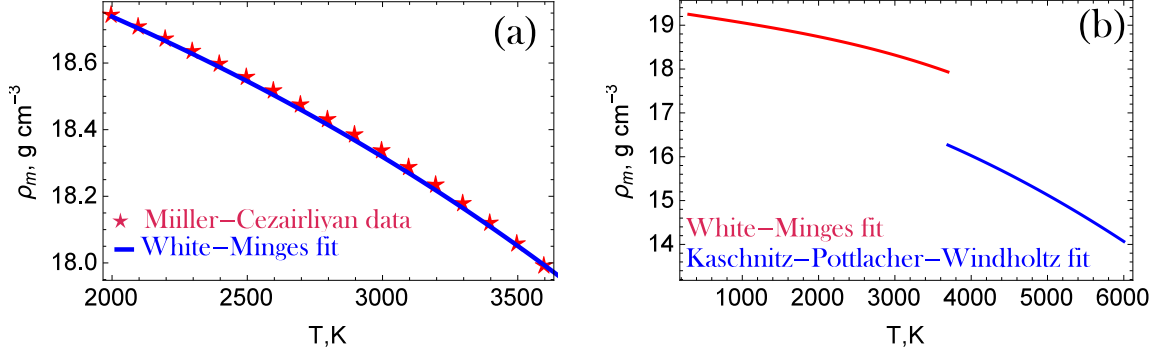


FIG. 10: (a) Comparison of the White–Minges fit close to the tungsten melting point,  $2000 < T(\text{K}) < 3695$ , with the dedicated high temperature measurements of Miiller and Cezairliyan [69]. (b) The complete recommended analytical description of the tungsten mass density from 300 to 6000 K.

**Recommended description.** In order to complete the description, it is necessary to verify that the White–Minges fit is reliable at high temperatures close to the melting point. Miiller and Cezairliyan had employed a precise high-speed interferometric technique for the measurement of the thermal expansion of tungsten from 1500 K up to the melting point [69]. The maximum uncertainty in the measured linear expansion was estimated to be  $\sim 1\%$  at 2000 K and  $\sim 2\%$  at 3600 K. From figure 10a, it is clear that their experimental results are nearly indistinguishable from the White–Minges fit. Overall, the recommended description comprises of the White–Minges fit in the temperature range  $300 < T(\text{K}) < 3695$  and the Kaschnitz–Pottlacher–Windholtz fit in the temperature range  $3695 < T(\text{K}) < 6000$ . See figure 10b for an illustration. From the above, we have  $\rho_m^s = 17.934 \text{ g cm}^{-3}$  and  $\rho_m^l = 16.267 \text{ g cm}^{-3}$ . The resulting discontinuity at the liquid-solid phase transition is  $\Delta\rho_m = 1.667 \text{ g cm}^{-3}$ . As expected we have  $\rho_m^s > \rho_m^l$  similar to most metals [45]. It is worth noting that the large relative magnitude of the discontinuity implies a rather large volume expansion during melting compared to other bcc metals [45].

## F. The surface tension

**Liquid metals.** Conventional techniques can be utilized for the measurement of the surface tension of liquid metals such as the maximum bubble pressure method, the sessile drop method and the pendant drop - drop weight method [70]. For melts of refractory metals, container-less (or non-contact) methods and particularly levitating drop methods are required in order to eliminate the possibility of chemical reactions between the melt and crucibles or substrates [71–73]. Different variants of the levitating drop method have been developed such as aerodynamic, optical, electrostatic and electromagnetic levitation [72, 73]. The experimental results originating from electrostatic levitation measurements are generally considered to be more accurate [71] due to the inherent advantages of this method [73, 74]. The electrostatic levitation method is based on lifting a small charged material sample with the aid of electrostatic fields, melting the sample with the aid of lasers, inducing shape oscillations by applying a small amplitude ac modulation to the field, recording the oscillating frequency as well as the amplitude damping of the drop shape profile, which

TABLE III: The surface tension of tungsten at the melting temperature according to dedicated experiments. The dataset of Allen [80] has been corrected for the liquid mass density following Ref.[82], since the exact experimental output in the pendant drop - drop weight method is the ratio  $\sigma/\rho_m$  and the room-temperature tungsten density was employed in the original work.

Investigators	Reference	Year	$\sigma_m$ (N/m)	Experimental method
Caverly	[79]	1957	2.300	pendant drop - drop weight
Allen	[80]	1963	2.355	pendant drop - drop weight
Martsenyuk <i>et al.</i>	[81]	1974	2.316	pendant drop - drop weight
Vinet <i>et al.</i>	[82]	1993	2.310	pendant drop - drop weight
Paradis <i>et al.</i>	[78]	2005	2.480	electrostatic levitation

provide the surface tension and the viscosity [74]. It is worth noting that the temperature dependence of the liquid metal surface tension has also been extensively studied because surface tension gradients (here caused by temperature gradients) can drive thermo-capillary Marangoni flows. In general, it is assumed that the dependence of the surface tension of pure liquid metals on the temperature is linear [70, 71, 73, 75]. This linearity is not imposed by theoretical arguments, but more likely stems from the limited temperature range of the experiments and the insufficient accuracy of the measurements. The basic constraint imposed by thermodynamics is that the surface tension reduces to zero at the critical point [45]. These remarks imply that the temperature coefficient is always negative; positive values have been measured but - most of the times - they can be attributed to impurity effects or non-equilibrium conditions [45].

**Liquid tungsten.** Numerous reviews dedicated to experimental measurements of the surface tension of liquid metals can be encountered in the literature [70, 71, 76, 77]. In these compilations, very few data can be found for the surface tension of tungsten at the melting point and no measurements can be found for the temperature dependence of the tungsten surface tension. Fortunately, very recent experiments were carried out by Paradis *et al.* with the electrostatic levitation method [78]. The surface tension was measured for liquid tungsten barely above the melting point and in the under-cooled phase,  $3360 < T(\text{K}) < 3700$ . The temperature interval of 350 K can be considered as adequate for the determination of the temperature coefficient. A linear fit of the form  $\sigma = \sigma_m - \beta(T - T_m)$  provided an accurate description of the data, which - in absence of other measurements - needs to be extrapolated in the entire liquid phase. The *Paradis fit* reads as [78]

$$\sigma = 2.48 - 0.31 \times 10^{-3}(T - T_m)$$

where  $\sigma$  is measured in N/m. The uncertainties in the least square fit coefficients are  $\sim 10\%$  ( $\sigma_m$ ) and  $\sim 25\%$  ( $\beta$ ). The surface tension at the melting point  $\sigma_m$  displays a strong agreement with previous measurements, as seen in Table III. We shall check how physical is the experimental value of the linear coefficient  $\beta$  by extrapolating at very high temperatures and determining the critical point temperature from  $\sigma = 0$ . The result is  $T_c \simeq 11700$  K. There is a remarkable agreement with numerous estimates of the tungsten critical point. In particular; the Guldberg rule leads to 12277 K, the Likalter equation of state leads to 12466 K, the Goldstein scaling leads to 11852 K and dynamic experiments using exploding wires lead on average to 12195 K [83].

### G. The dynamic viscosity

**Liquid metals.** Conventional techniques can be employed for the measurement of the dynamic viscosity of liquid metals such as the capillary method, the oscillating vessel method and the rotating cylinder method [45, 84, 85]. For melts of refractory metals, non-contact techniques such as the electrostatic levitation method are preferred due to the high melting temperatures and the enhanced reactivity at elevated temperatures [86, 87]. In general, it is assumed that the dependence of the dynamic viscosity of pure liquid metals on the temperature is of the Arrhenius form [45, 75], *i.e.*  $\mu(T) = \mu_0 \exp[E_a/(RT)]$  with  $E_a$  the activation energy for viscous flow,  $\mu_0$  the pre-exponential viscosity and  $R = 8.314$  J/(mol·K) the ideal gas constant. It should also be emphasized that, within some limitations, the dynamic viscosity and the surface tension are connected by a rigorous statistical mechanics relation. The Fowler formula for the surface tension of liquids reads as  $\sigma = (\pi n^2/8) \int_0^\infty r^4 g(r) [d\phi(r)/dr] dr$ , where  $g(r)$  is the pair correlation function,  $\phi(r)$  is the pair interaction potential and  $n$  is the particle number density [88, 89]. The Born-Green formula for the viscosity of liquids reads as  $\mu = \sqrt{m/(k_B T)} (2\pi n^2/15) \int_0^\infty r^4 g(r) [d\phi(r)/dr] dr$ , with  $m$  the particle atomic mass [90]. Dividing by parts, the Fowler-Born-Green formula emerges,  $\mu(T) = (16/15) \sqrt{m/(k_B T)} \sigma(T)$  [91–93]. The fundamental assumptions behind the Fowler formula and the Born-Green formula determine the applicability range of this particularly simple elegant formula [93]: (i) three particle correlations are neglected, which implies that the formulas are not valid for rapid supercooling that brings the liquid system close to the glass transition point, (ii) contributions

from the soft long-range part of the potential are neglected, which implies that the formulas are essentially derived within a hard sphere model and that they are valid for systems characterized by short-range isotropic interactions such as liquid metals, (iii) pure elements are considered, which implies that the formulas are not valid for alloys.

**Liquid tungsten.** Numerous works that have reviewed experimental data for the viscosity of liquid metals, elemental or alloys, can be encountered in the literature [39, 75, 94–96]. Similar to the case of surface tension, in these compilations, very few data can be found for the viscosity of tungsten at the melting point and no measurements for its temperature dependence. Fortunately, very recent experiments were carried out by Ishikawa *et al.* with the electrostatic levitation method [97, 98]. The measurements reported in Ref.[98] will be considered in greater detail, since it has been concluded that the measurements of Ref.[97] were affected by sample positioning forces. In Ref.[98], the viscosity was measured for liquid tungsten in the under-cooled phase,  $3155 < T(\text{K}) < 3634$ . The temperature interval of 480 K can be considered as adequate for the determination of the temperature dependence. An Arrhenius fit of the form  $\mu = \mu_0 \exp [E_a/(RT)]$  provided an accurate description of the data, which - in absence of other measurements - needs to be extrapolated in the entire liquid phase. The *Ishikawa fit* reads as [98]

$$\mu = 0.16 \times 10^{-3} \exp \left( 3.9713 \frac{T_m}{T} \right),$$

where  $\mu$  is measured in Pas. This expression corresponds to an activation energy  $E_a = 122 \times 10^3 \text{ J/mol}$  which has been determined by least square fitting with a 20% uncertainty. The extrapolated value of the viscosity at the melting point is  $\mu(T_m) = 8.5 \times 10^{-3} \text{ Pas}$  close to the experimental value  $\mu(T_m) = 7.0 \times 10^{-3} \text{ Pas}$  provided in the literature [75]. Both measurements of Ishikawa *et al.* [97, 98] are illustrated in figure 11a together with the least square fitted Arrhenius expressions. In the absence of other experimental results, the Fowler-Born-Green formula provides the only way to cross-check the adopted measurements. In figure 11b, the ratio of  $\sigma(T)/\mu(T)$ , where  $\sigma(T)$  follows the Paradis fit and  $\mu(T)$  follows the Ishikawa fit, is expressed in units of  $(15/16)\sqrt{(k_B T)/m}$  and plotted as a function of the temperature. The quantity does not diverge strongly from unity, especially taking into account the experimental uncertainties and the wide extrapolations in the viscosity as well as the surface tension. It is worth investigating whether fitting expressions other than the pure Arrhenius form can equally fit the experimental data, but provide a better agreement with the Fowler-Born-Green formula. A cubic Arrhenius fit,

$$\mu = 2.76 \times 10^{-3} \exp \left[ 1.1362 \left( \frac{T_m}{T} \right)^3 \right],$$

where  $\mu$  is measured in Pas, fulfills these two criteria. It is impossible to determine whether the extrapolated Arrhenius fit for the viscosity or the extrapolated linear fit for the surface tension are responsible for the deviations from the Fowler-Born-Green formula, not to mention that this formula should not be exactly obeyed across the liquid phase. Therefore, we still recommend the use of the pure Arrhenius fit. The aim of this comparison was to highlight the need for tungsten surface tension and viscosity measurements in larger temperature ranges and for temperatures exceeding the melting point.

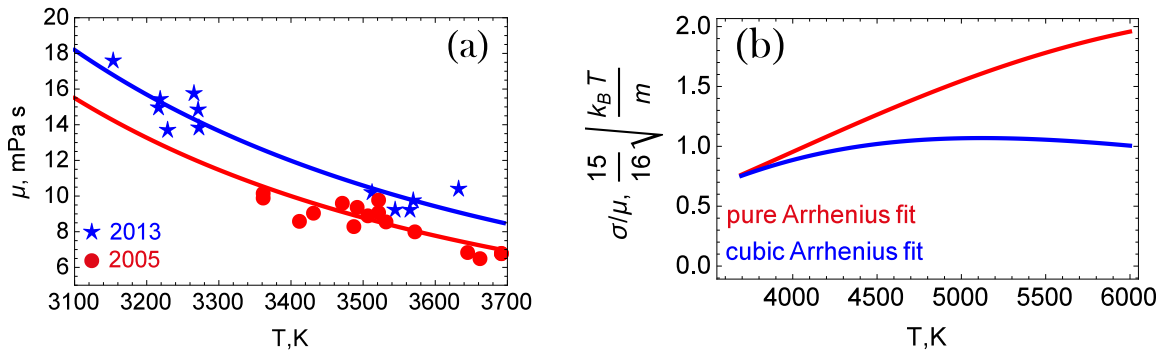


FIG. 11: (a) The viscosity of liquid tungsten in the under-cooled phase; experimental results and Arrhenius least square fits [97, 98]. (b) The validity of the Fowler-Born-Green formula across the liquid phase of tungsten adopting the linear expression for the surface tension and either a pure Arrhenius or a cubic Arrhenius expression for the viscosity.



### III. RECOMMENDED ANALYTICAL EXPRESSIONS

As aforementioned, the thermophysical properties analyzed above constitute input for simulations of the response of tungsten plasma-facing components (or tungsten dust) to incident plasma heat loads. In this section, in lieu of conclusions, it was judged to be more practical for the specialized reader that we simply gather the recommended analytical expressions for the temperature dependence of the thermophysical properties of pure solid and liquid tungsten. For the **latent heat of fusion**, we recommend the typical literature value of

$$\Delta h_f = 52.3,$$

where  $\Delta h_f$  is measured in kJ/mol. For the **electrical resistivity**, we recommend the White–Minges fit in the temperature range  $100 \leq T(\text{K}) \leq 3695$  and the Seydel–Fücke fit in the temperature range  $3695 \leq T(\text{K}) \leq 6000$ ,

$$\rho(T) = \begin{cases} -0.9680 + 1.9274 \times 10^{-2}T + 7.8260 \times 10^{-6}T^2 - 1.8517 \times 10^{-9}T^3 + 2.0790 \times 10^{-13}T^4 & 100 \leq T(\text{K}) \leq 3695, \\ 135 - 1.855 \times 10^{-3}(T - T_m) + 4.420 \times 10^{-6}(T - T_m)^2 & 3695 \leq T(\text{K}) \leq 6000, \end{cases}$$

where  $\rho$  is measured in  $10^{-8} \Omega\text{m}$  or in  $\mu\Omega\text{cm}$ . For the **specific isobaric heat capacity**, we recommend the White–Minges fit in the temperature range  $300 \leq T(\text{K}) \leq 3080$ , the Wilthan *et al.* fit in the temperature range  $3080 \leq T(\text{K}) \leq 3695$  and the Wilthan *et al.* value in the temperature range  $T(\text{K}) \geq 3695$ ,

$$c_p(T) = \begin{cases} 21.868372 + 8.068661 \times 10^{-3}T - 3.756196 \times 10^{-6}T^2 + 1.075862 \times 10^{-9}T^3 + \frac{1.406637 \times 10^4}{T^2} & 300 \leq T(\text{K}) \leq 3080 \\ 2.022 + 1.315 \times 10^{-2}T & 3080 \leq T(\text{K}) \leq 3695 \\ 51.3 & T(\text{K}) \geq 3695 \end{cases}$$

where  $c_p$  is measured in J/(mol K). For the **thermal conductivity**, we recommend the modified Hust–Lankford fit in the temperature range  $300 < T(\text{K}) < 3695$  and the Seydel–Fücke fit in the temperature range  $3695 < T(\text{K}) < 6000$ ,

$$k(T) = \begin{cases} 149.441 - 45.466 \times 10^{-3}T + 13.193 \times 10^{-6}T^2 - 1.484 \times 10^{-9}T^3 + \frac{3.866 \times 10^6}{T^2} & 300 \leq T(\text{K}) \leq 3695 \\ 66.6212 + 0.02086(T - T_m) - 3.7585 \times 10^{-6}(T - T_m)^2 & 3695 \leq T(\text{K}) \leq 6000, \end{cases}$$

where  $k$  is measured in W/(m K). For the **mass density**, we recommend the White–Minges fit in the temperature range  $300 < T(\text{K}) < 3695$  and the Kaschnitz–Pottlacher–Windholz fit in the temperature range  $3695 < T(\text{K}) < 6000$ ,

$$\rho_m(T) = \begin{cases} 19.25 - 2.66207 \times 10^{-4}(T - T_0) - 3.0595 \times 10^{-9}(T - T_0)^2 - 9.5185 \times 10^{-12}(T - T_0)^3 & 300 \leq T(\text{K}) \leq 3695, \\ 16.267 - 7.679 \times 10^{-4}(T - T_m) - 8.091 \times 10^{-8}(T - T_m)^2 & 3695 \leq T(\text{K}) \leq 6000, \end{cases}$$

where  $\rho_m$  is measured in  $\text{g cm}^{-3}$  and  $T_0 = 293.15 \text{ K}$ . For the **surface tension**, we recommend the extrapolated linear Paradis fit

$$\sigma(T) = 2.48 - 0.31 \times 10^{-3}(T - T_m) \quad T(\text{K}) \geq 3695,$$

where  $\sigma$  is measured in N/m. For the **dynamic viscosity**, we recommend the extrapolated Arrhenius Ishikawa fit

$$\mu(T) = 0.16 \times 10^{-3} \exp\left(3.9713 \frac{T_m}{T}\right) \quad T(\text{K}) \geq 3695,$$

where  $\mu$  is measured in Pas.

- 
- [1] R. A. Pitts, A. Kukushkin, A. Loarte, A. Martin *et al.*, *Phys. Scr.* **T138**, 014001 (2009)
  - [2] R. A. Pitts, S. Carpentier, F. Escourbiac, T. Hirai *et al.*, *J. Nucl. Mater.* **438**, S48 (2013)
  - [3] G. Pintsuk, *Comprehensive Nuclear Materials* **4**, 551 (2012)
  - [4] I. Smid, M. Akiba, G. Vieider and L. Plöchl, *J. Nucl. Mater.* **258-263**, 160 (1998)
  - [5] J. W. Davis, V. R. Barabash, A. Makhankov, L. Plöchl and K. T. Slattery, *J. Nucl. Mater.* **258-263**, 308 (1998)
  - [6] V. Barabash *et al.*, *J. Nucl. Mater.* **367-370**, 21 (2007)

- [7] J. W. Coenen, V. Philipps, S. Brezinsek, B. Bazylev *et al.*, *Nucl. Fusion* **51**, 083008 (2011)
- [8] J. W. Coenen, G. Arnoux, B. Bazylev, G. F. Matthews *et al.*, *Nucl. Fusion* **55**, 023010 (2015)
- [9] B. Bazylev, G. Janeschitz, I. Landman, S. Pestchanyi *et al.*, *Fusion Eng. Des.* **83**, 1077 (2008)
- [10] B. Bazylev, G. Janeschitz, I. Landman, A. Loarte *et al.*, *J. Nucl. Mater.* **390-391**, 810 (2009)
- [11] G. Miloshevsky and A. Hassanein, *Nucl. Fusion* **54**, 043016 (2014)
- [12] S. I. Krasheninnikov, R. D. Smirnov and D. L. Rudakov, *Plasma Phys. Control Fus.* **53**, 083001 (2011)
- [13] L. Vignitchouk, P. Talias and S. Ratynskaia, *Plasma Phys. Control Fus.* **56**, 095005 (2014)
- [14] S. Ratynskaia, P. Talias, I. Bykov, D. Rudakov *et al.*, *Nucl. Fus.* **56**, 066010 (2016)
- [15] I. Egry, A. Diefenbach, W. Dreier and J. Piller, *Int. J. Thermophys.* **22**, 569 (2001)
- [16] T. Ishikawa, J. T. Okada, P.-F. Paradis and Y. Watanabe, *Jpn. J. Appl. Phys.* **50**, 11RD03 (2011)
- [17] S. V. Lebedev, A. I. Savvatimskii and Yu. B. Smirnov, *High Temp. (USSR)* **9**, 578 (1971)
- [18] M. M. Martynyuk, I. Karimkhodzhaev and V. I. Tsapkov, *Sov. Phys. Tech. Phys.* **19**, 1458 (1975)
- [19] J. W. Shaner, G. R. Gathers and C. Minichino, *High Temp. High Press.* **8**, 425 (1976)
- [20] U. Seydel, H. Bauhof, W. Fucke and H. Wadle, *High Temp. High Press.* **11**, 635 (1979)
- [21] D. W. Bonnell, in *Materials Measurements*, J. R. Manning, ed. (NBS Internal Report 83-2772, 1983)
- [22] E. Arpacı and M. G. Froberg, *Z. Metallkde.* **75**, 614 (1984)
- [23] A. Berthault, L. Arles and J. Matricon, *Int. J. Thermophys.* **7**, 167 (1986)
- [24] V. N. Senchenko and M. A. Sheindlin, *High Temp. (USSR)* **25**, 364 (1987)
- [25] R. S. Hixson and M. A. Winkler, *Int. J. Thermophys.* **11**, 709 (1990)
- [26] E. Kaschnitz, G. Pottlacher and L. Windholz, *High Press. Res.* **4**, 558 (1990)
- [27] J. L. McClure and A. Cezairliyan, *Int. J. Thermophys.* **14**, 449 (1993)
- [28] G. Pottlacher, E. Kaschnitz and H. Jäger, *J. Non-Cryst. Solids* **156-158**, 374 (1993)
- [29] N. I. Kuskova, S. I. Tkachenko and S. V. Koval, *Int. J. Thermophys.* **19**, 341 (1998)
- [30] P. Gustafson, *Int. J. Thermophys.* **6**, 395 (1985)
- [31] G. Grimvall, M. Thiessen and A. F. Guillermet, *Phys. Rev. B* **36**, 7816 (1987)
- [32] A. T. Dinsdale, *CALPHAD* **15**, 317 (1991)
- [33] E. Lassner and W.-D. Schubert, *Tungsten: Properties, Chemistry, Technology of the Element, Alloys, and Chemical Compounds* (Springer, Berlin, 1999)
- [34] D. R. Lide, *CRC Handbook of Chemistry and Physics* (CRC Press, Boca Raton, 2004)
- [35] W. Martienssen and H. Warlimont, *Springer Handbook of Condensed Matter and Materials Data* (Springer, Berlin, 2005)
- [36] F. Cardarelli, *Materials Handbook: A Concise Desktop Reference* (Springer-Verlag, London, 2008)
- [37] I. L. Shabalin, *Ultra-high Temperature Materials I* (Springer, Dordrecht, 2014)
- [38] C. Cagran and G. Pottlacher, *Dynamic pulse calorimetry - Thermophysical properties of solid and liquid metals and alloys in Handbook of Thermal Analysis and Calorimetry Vol. 5: Recent Advances, Techniques and Applications* eds. M. E. Brown and P. K. Gallagher (Elsevier, Amsterdam, 2005)
- [39] G. V. Samsonov, *Handbook of the Physicochemical Properties of the Elements* (Plenum, New York, 1968)
- [40] G. Grimvall, *Thermophysical properties of materials* (Elsevier, Amsterdam, 1999)
- [41] M. E. Glicksman, *Principles of Solidification* (Springer, New York, 2011)
- [42] P. D. Desai, T. K. Chu, H. M. James and C. Y. Ho, *J. Phys. Chem. Ref. Data* **13**, 1069 (1984)
- [43] G. K. White and M. L. Mingos, *Int. J. Thermophys.* **18**, 1269 (1997)
- [44] L. Vignitchouk, *Modelling the multifaceted physics of metallic dust and droplets in fusion plasmas* (PhD Thesis, KTH Stockholm, 2016)
- [45] T. Iida and R. Guthrie, *The Thermophysical Properties of Metallic Liquids Volume 1: Fundamentals* (Oxford University Press, Oxford, 2015)
- [46] U. Seydel and W. Fucke, *J. Phys. F: Metal Phys.* **10**, L203 (1980)
- [47] B. Wilthan, C. Cagran and G. Pottlacher, *Int. J. Thermophys.* **26**, 1017 (2005)
- [48] T. Hüpf, C. Cagran, G. Lohöfer and G. Pottlacher, *J. Phys. Conf. Ser.* **98**, 062002 (2008)
- [49] T. Hüpf, C. Cagran and G. Pottlacher, *EPJ Web Conf.* **15**, 01018 (2011)
- [50] M. W. Chase, NIST-JANAF Thermochemical Tables (Fourth Edition), *J. Phys. Chem. Ref. Data Monograph* **9**, 1 (1998)
- [51] <http://webbook.nist.gov>
- [52] G. K. White and S. J. Collocott, *J. Phys. Chem. Ref. Data* **13**, 1251 (1984)
- [53] I. Barin, *Thermochemical Data of Pure Substances* (VCH, Weinheim, 1995)
- [54] C. Y. Ho, R. W. Powell and P. E. Liley, *J. Phys. Chem. Ref. Data* **1**, 279 (1972)
- [55] C. Y. Ho, R. W. Powell and P. E. Liley, *J. Phys. Chem. Ref. Data* **3**, Suppl. 1 (1974)
- [56] J. G. Hust and A. B. Lankford, *Thermal Conductivity of Aluminum, Copper, Iron and Tungsten for Temperatures from 1 K to the Melting Point*: NBS Internal Report 84-3007 (U.S. Department of Commerce, Boulder, 1984)
- [57] A. A. Abrikosov, *Fundamentals of the Theory of Metals* (Elsevier, Amsterdam, 1988)
- [58] K. C. Mills, B. J. Monaghan and B. J. Keene, *Int. Mater. Rev.* **41**, 209 (1996)
- [59] M. Boivineau and G. Pottlacher, *Int. J. Mater. Prod. Tec.* **26**, 217 (2006)
- [60] F. Seitz, *The Modern Theory of Solids* (McGraw-Hill, New York, 1940)
- [61] C. Kittel, *Introduction to Solid-State Physics* (John Wiley & Sons, New Jersey, 2005)
- [62] G. Pottlacher, *J. Non-Cryst. Solids* **250-252**, 177 (1999)
- [63] H. Hess, A. Kloss, A. Rakhel and H. Schneidenbach, *Int. J. Thermophys.* **20**, 1279 (1999)
- [64] A. V. Grosse, *J. Inorg. Nucl. Chem.* **28**, 795 (1966)

- [65] A. V. Grosse, *J. Inorg. Nucl. Chem.* **28**, 803 (1966)
- [66] U. Seydel and W. Kitzel, *J. Phys. F: Metal Phys.* **9**, L153 (1979)
- [67] G. R. Gathers, *Rep. Prog. Phys.* **49**, 341 (1986)
- [68] V. V. Ivanov, S. V. Lebedev and A. I. Savvatimskii, *J. Phys. F: Metal Phys.* **14**, 1641 (1984)
- [69] A. P. Müller and A. Cezairliyan, *Int. J. Thermophys.* **12**, 643 (1991)
- [70] B. J. Keene, *Int. Mater. Rev.* **38**, 157 (1993)
- [71] K. C. Mills and Y. C. Su, *Int. Mater. Rev.* **51**, 329 (2006)
- [72] I. Egry, E. Ricci, R. Novakovic and S. Ozawa, *Adv. Colloid Interface Sci.* **159**, 198 (2010)
- [73] P.-F. Paradis, T. Ishikawa, G.-W. Lee, D. Holland-Moritz, J. Brillo, W.-K. Rhim and J. T. Okada, *Mater. Sci. Eng. R Rep.* **76**, 1 (2014)
- [74] W.-K. Rhim, K. Ohsaka, P.-F. Paradis and R. E. Spjut, *Rev. Sci. Instrum.* **70**, 2796 (1999)
- [75] T. Iida and R. Guthrie, *The Thermophysical Properties of Metallic Liquids Volume 2: Predictive Models* (Oxford University Press, Oxford, 2015)
- [76] O. Flint, *J. Nucl. Mater.* **16**, 233 (1964)
- [77] D. W. G. White, *Metall. Rev.* **13**, 73 (1968)
- [78] P.-F. Paradis, T. Ishikawa, R. Fujii and S. Yoda, *Appl. Phys. Lett.* **86**, 041901 (2005)
- [79] A. Calverley, *Proc. Phys. Soc.* **70B**, 1040 (1957)
- [80] B. C. Allen, *Trans. AIME* **227**, 1175 (1963)
- [81] P. S. Martsenyuk, Yu. N. Ivashchenko and V. N. Eremenko, *High Temp.* **12**, 1310 (1974)
- [82] B. Vinet, J. P. Garandet and L. Cortella, *J. Appl. Phys.* **73**, 3830 (1993)
- [83] H. Hess, *Phys. Chem. Liq.* **30**, 251 (1995)
- [84] R. F. Brooks, A. T. Dinsdale and P. N. Quested, *Meas. Sci. Technol.* **16** 354 (2005)
- [85] J. Cheng, J. Gröbner, N. Hort, K. U. Kainer and R. Schmid-Fetzer, *Meas. Sci. Technol.* **25** 062001 (2014)
- [86] T. Ishikawa, P.-F. Paradis, T. Itami and S. Yoda, *J. Chem. Phys.* **118**, 7912 (2003)
- [87] T. Ishikawa, P.-F. Paradis, J. T. Okada and Y. Watanabe, *Meas. Sci. Technol.* **23** 025305 (2012)
- [88] R. H. Fowler, *Proc. Roy. Soc. A* **159**, 229 (1937)
- [89] J. G. Kirkwood and F. P. Buff, *J. Chem. Phys.* **17**, 338 (1949)
- [90] M. Born and H. S. Green, *Proc. Roy. Soc. A* **190**, 455 (1947)
- [91] I. Egry, *Scr. Metall. Mater.* **26**, 1349 (1992)
- [92] I. Egry, G. Lohöfer and S. Sauerland, *J. Non-Cryst. Solids* **156-158**, 830 (1993)
- [93] I. Egry, *Scr. Metall. Mater.* **28**, 1273 (1993)
- [94] L. Battezzati and A. L. Greer, *Acta Metall.* **37**, 1791 (1989)
- [95] R. P. Chhabra and D. K. Sheth, *Z. Metallkd.* **81**, 264 (1990)
- [96] T. Iida, R. Guthrie, M. Isac and N. Tripathi, *Metall. Mater. Trans. B* **37**, 403 (2006)
- [97] P.-F. Paradis, T. Ishikawa and S. Yoda, *J. Appl. Phys.* **97**, 106101 (2005)
- [98] T. Ishikawa, P.-F. Paradis, J. T. Okada, M. V. Kumar and Y. Watanabe, *J. Chem. Thermodyn.* **65**, 1 (2013)